Letter

Observing Floquet topological order by symmetry resolution

Daniel Azses,[1] Emanuele G. Dalla Torre,[2,3] and Eran Sela[1]
[1]*School of Physics and Astronomy, Tel Aviv University, Tel Aviv 6997801, Israel*
[2]*Department of Physics, Bar-Ilan University, Ramat Gan 5290002, Israel*
[3]*Center for Quantum Entanglement Science and Technology, Bar-Ilan University, Ramat Gan 5290002, Israel*

(Received 14 September 2021; accepted 16 November 2021; published 2 December 2021)

Symmetry-protected topological order in one dimension leads to protected degeneracies between symmetry blocks of the reduced density matrix. In the presence of periodic driving, topological Floquet phases can be identified in terms of a cycling of these symmetry blocks between different charge quantum numbers. We discuss an example of this phenomenon with an Ising $\mathbb{Z}_2$ symmetry, using both analytic methods and real quantum computers. By adiabatically moving along the phase diagram, we demonstrate that the cycling periodicity is broken in Floquet topological phase transitions. An equivalent signature of the topological Floquet phase is identified as a computational power allowing for the teleportation of quantum information.

DOI: 10.1103/PhysRevB.104.L220301

Introduction. Floquet symmetry-protected topological (FSPT) phases are emergent condensed matter phenomena [1–9] that extend the concept of symmetry-protected topological (SPT) order to periodically driven systems [10–13]. A key aspect of one-dimensional (1D) SPTs is having ground states with protected degeneracies in their entanglement spectrum [14–18]. For unitary symmetries, these degeneracies can be detected with symmetry-resolved entanglement (SRE) measures [19–27], and allow one to use SPTs as universal computational resources [28–30]. Whether and how these properties show up for FSPT order are the questions that we address in this Letter.

In periodically driven systems, the key object that admits topological features is the unitary Floquet operator describing the time evolution for one cycle, $F = U(T, 0)$, where T is the time period. Its eigenvalues, $\lambda_i = e^{-iT\varepsilon_i}$, which define the quasienergies $\omega_i = T\varepsilon_i \bmod 2\pi$, have topological characteristics such as protected 0- and/or π-edge modes [2]. In contrast to static SPTs, the eigenstates of F are not necessarily entangled, even in nontrivial FSPTs. Instead, entanglement in FSPTs is hidden in the time evolution within a period, which is often referred to as *micromotion* and is generically characterized by quantized charge pumping [5,31]. Here, we study and experimentally observe this phenomenon by focusing on the dynamics of the SRE, derived from the block diagonal structure of the reduced density matrix $\rho_A = \mathrm{Tr}_B\, \rho$ [17]. In the static case, the SRE structure can be used to identify SPT phases via degeneracies between the symmetry blocks [16]. Our key observation here is that nontrivial FSPT order is reflected by an exact cycling of the symmetry blocks upon Floquet evolution, as illustrated in Fig. 1. As an experimentally detectable [16,32] consequence, the first moment of the SRE, defined as the subsystem charge, displays cyclic switching. This is demonstrated for a $\mathbb{Z}_2$ FSPT phase on a noisy intermediate-scale quantum (NISQ) computer. We quantify the parity switching as an order parameter, and observe its dynamics across a Floquet topological phase transition. We propose a generalization of measurement-based quantum computation (MBQC) to the FSPT case. Lastly, static SPT order can also coexist with nontrivial Floquet order, in which case the protected entanglement is associated with degeneracies between cyclically switching symmetry blocks.

Cohomological classification. Before discussing our main result, we put it in the mathematical context of the classification of 1D bosonic SPTs. A 1D SPT phase protected by the symmetry group G is characterized by a ground state accompanied by a symmetry operator $U(g)$ representing the group G. While $U(g)$ acts on the full system as a conventional representation, it acts near the edges [28,33] via a projective representation that classifies the different SPT phases into $\mathcal{H}^2[G, U(1)]$ classes [13].

One-dimensional bosonic FSPTs are characterized by an additional discrete symmetry, namely translations in time by integer multiples of the period, or equivalently, discrete powers of F. Because this operator commutes with the static symmetry G, the total system is characterized by a $G \times \mathbb{Z}$ symmetry. As a result, there are $\mathcal{H}^2[G \times \mathbb{Z}, U(1)]$ bosonic FSPT phases [4,5,34]. For finite Abelian groups G we find that [35] (see also Refs. [36–38] therein)

$$\mathcal{H}^2[G \times \mathbb{Z}, U(1)] = \mathcal{H}^2[G, U(1)] \times G. \tag{1}$$

One can understand the two factors in Eq. (1) as a bulk SPT order classified by $\mathcal{H}^2[G, U(1)]$, which results in degeneracies between the symmetry blocks of ρ_A, and additional $|G|$ phases that characterize the possible cyclic permutations of the SRE, after applying F. Importantly, even symmetry groups whose cohomology group is trivial and cannot support static SPT phases can protect nontrivial Floquet topology.

SRE switching. For a system characterized by a unitary symmetry G with a conserved charge $\mathcal{Q}_{\mathrm{tot}}$, the density matrix of the reduced system A has a decomposition [39] $\rho_A = \oplus_{\mathcal{Q}} \tilde{\rho}_A(\mathcal{Q})$ associated with subsystem charge $\mathcal{Q} \equiv \mathcal{Q}_A$. We

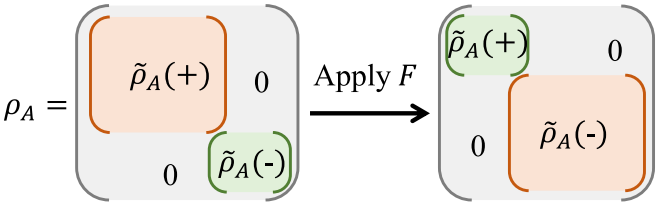

FIG. 1. FSPT order is characterized by cyclic switching of symmetry blocks of the reduced density matrix upon applying the Floquet operator $F = U(T, 0)$.

define the nth Rényi SRE as $S_n(\mathcal{Q}) = \mathrm{Tr}[\Pi_\mathcal{Q}\rho_A^n]$, where $\Pi_\mathcal{Q}$ projects subsystem A to charge sector $\mathcal{Q}$. For example, for the symmetry group $G = \mathbb{Z}_N$, the charge $\mathcal{Q}$ is an integer, modulo N. This group has a trivial cohomology group $\mathcal{H}^2[\mathbb{Z}_N, U(1)]$ and hence cannot support static SPTs. According to Eq. (1), we have exactly $|\mathbb{Z}_N| = N$ distinct FSPT phases. Each phase is labeled by an integer $c = 0, 1, \ldots, N-1$, which represents the pumped charge of the FSPT phase. Let us focus on eigenstates of the Floquet operator in the bulk, but not necessarily on the edges. After one cycle $\rho \to \rho' = F\rho F^\dagger$, and, as we now demonstrate,

$$S_n(\mathcal{Q}) \to S_n'(\mathcal{Q}) = \mathrm{Tr}[{\rho_A'}^n \Pi_\mathcal{Q}] = S_n(\mathcal{Q}'), \tag{2}$$

where $\mathcal{Q}' = \mathcal{Q} + c$. Equation (2) tells us that the symmetry sector $\mathcal{Q}$ goes to $\mathcal{Q}'$ upon acting with F. Being valid for any n, this relation implies the cycling of the entire spectrum of each symmetry block $\tilde{\rho}_A(\mathcal{Q})$, as schematically shown in Fig. 1.

We now prove this result using the framework of Ref. [6]. Assuming that the FSPT phase with symmetry G is integrable or many-body localized (MBL) (see Refs. [41–43]), we have an edge-bulk decomposition of the one-period time evolution operator

$$F = v_L v_R e^{-if}, \tag{3}$$

where v_L (v_R) is a unitary operator localized at the left (right) part of the system and f is a functional of the symmetric (with respect to G) constants of motion associated with the MBL [6]. Additionally, we have the identity

$$\begin{aligned} U(g) v_L U^\dagger(g) v_L^\dagger &= \kappa_c(g), \\ U(g) v_R U^\dagger(g) v_R^\dagger &= \kappa_c^{-1}(g), \end{aligned} \tag{4}$$

for unitary symmetries represented by $U(g)$, where $g \in G$ and $\kappa_c(g)$ is the 1D representation of the FSPT matching the group element c such that $U(c)|g\rangle = \kappa_c(g)|g\rangle$ [6]. As the state is an eigenstate of F in the bulk, it is an eigenstate of e^{-if}. If we consider Floquet phases that do not break any symmetry (including time translations) the state is an eigenstate of e^{-if} and this phase factor drops out of the evolved state $\rho' = F\rho F^\dagger = v_L v_R \rho v_R^\dagger v_L^\dagger$ [6].

We now calculate the first moment $S_1(\mathcal{Q}) = \mathrm{Tr}[\Pi_\mathcal{Q}\rho_A]$ of the SRE, which is the probability that the reduced system has charge $\mathcal{Q}$. For Abelian unitary finite symmetries, the projectors can be written in terms of the group characters $\chi_\mathcal{Q}(g)$ [18,44],

$$\Pi_\mathcal{Q} = \frac{1}{|G|} \sum_{g\in G} \chi_\mathcal{Q}(g) U_A(g), \tag{5}$$

where $U_A(g)$ is the symmetry acting on the reduced system A. If subsystem A includes the left but not the right edge, we have that $\rho_A \to \rho_A' = v_L \rho_A v_L^\dagger$ and $\Pi_\mathcal{Q}$ commutes with v_R. Thus, after one cycle $S_1(\mathcal{Q}) \to S_1'(\mathcal{Q}) = \mathrm{Tr}[v_L^\dagger \Pi_\mathcal{Q} v_L \rho_A] = \frac{1}{|G|}\sum_{g\in G} \chi_\mathcal{Q}(g)\mathrm{Tr}[v_L^\dagger U_A(g) v_L \rho_A]$. Using the identity $v_L^\dagger U_A(g) v_L = \kappa_c(g) U_A(g)$, which derives from Eq. (4) by partial tracing, we obtain

$$v_L^\dagger \Pi_\mathcal{Q} v_L = \Pi_{\mathcal{Q}+c}. \tag{6}$$

Then Eq. (2) follows for the case $n = 1$. Generalizing this result to any n is straightforward: After one cycle, we have that $\rho_A^n \to (v_L \rho_A v_L^\dagger)^n = v_L \rho_A^n v_L^\dagger$ as v_L is unitary and satisfies $v_L^\dagger v_L = I$. As a result, the nth Rényi SRE evolves as $S_n(\mathcal{Q}) = \mathrm{Tr}[\Pi_\mathcal{Q}\rho_A^n] \to S_n'(\mathcal{Q}) = \mathrm{Tr}[v_L^\dagger \Pi_\mathcal{Q} v_L \rho_A^n] = \frac{1}{|G|}\sum_{g\in G}\chi_\mathcal{Q}(g)\mathrm{Tr}[v_L^\dagger U_A(g) v_L \rho_A^n]$. Together with the assumptions and derivations above, this proves Eq. (2) for any n.

Parity switching through a phase transition. The subsystem charge can serve as a measurable order parameter of FSPT phases that can be observed even on small noisy quantum computers. We now study its evolution across a phase transition.

To showcase the use of this order parameter, we consider the kicked Ising model $F(\alpha, \beta) = U_{ZZ}(\beta)U_X(\alpha)$ where

$$\begin{aligned} U_X(\alpha) &= e^{i\frac{\alpha}{2}\sum_{l=1}^{L} X_l}, \\ U_{ZZ}(\beta) &= e^{i\frac{\beta}{2}\sum_{l=1}^{L-1} Z_l Z_{l+1}}, \end{aligned} \tag{7}$$

and X_l, Z_l are Pauli matrices acting on the lth site of a chain with open boundary conditions. This model has a $G = \mathbb{Z}_2$ symmetry represented by the parity operator $P = \prod_{l=1}^{L} X_l$. Its phase diagram [40] is displayed in Fig. 2(a). The four phases are labeled by the number of single Majorana fermion excitations at quasienergies 0 and π [see Fig. 2(b)]. The phases with an odd number of Majoranas spontaneously break the Ising symmetry, and correspond to a ferromagnet (0 phase) and to a time crystal (π phase) [45–48]. The latter phase was realized using trapped ions [49] and superconducting circuits [48,50–52]. The Floquet topological phase 0π was realized in Ref. [8] using cold atoms.

Here, we focus on the transition from the FSPT (0π) phase to the ferromagnetic (0) phase. The former phase has two interconnected properties: protected edge states at quasienergy π and SRE swapping. The probability of the even subsystem parity $S_1(\mathrm{even}) = \frac{1+\langle P_A\rangle}{2}$ [with $S_1(\mathrm{odd}) = 1 - S_1(\mathrm{even})$] is obtained by evaluating the subsystem parity $P_A = \prod_{i\in A} X_i$ where A includes L_A sites from the left boundary. In the topological phase, $S_1(\mathrm{even})$ and $S_1(\mathrm{odd})$ are expected to swap their values at each time step. This behavior is trivially seen, for example, at the sweet spot $\beta = \pi$ and $\alpha = 0$ where $U_{ZZ}(\pi) = (-i)^{L-1} Z_1 Z_L$ and $U_X = 1$. Then the evolution over one period $F = U_{ZZ}U_X$ simply flips the two edges from $+$ to $-$ and $S_1(\mathrm{even})$ and $S_1(\mathrm{odd})$ alternate between 0 and 1.

To see that this property persists in the entire topological phase, but disappears in the ferromagnetic phase, we adiabatically change the parameters of F. Specifically, we follow the path $\alpha = r_0 \cos\theta$ and $\beta = \pi - r_0 \sin\theta$, shown as a red curve in Fig. 2(a), in N_steps equal steps, such that the topological phase transition is crossed at $\theta = \pi/4$, i.e., at the $N_\mathrm{steps}/2$ step.

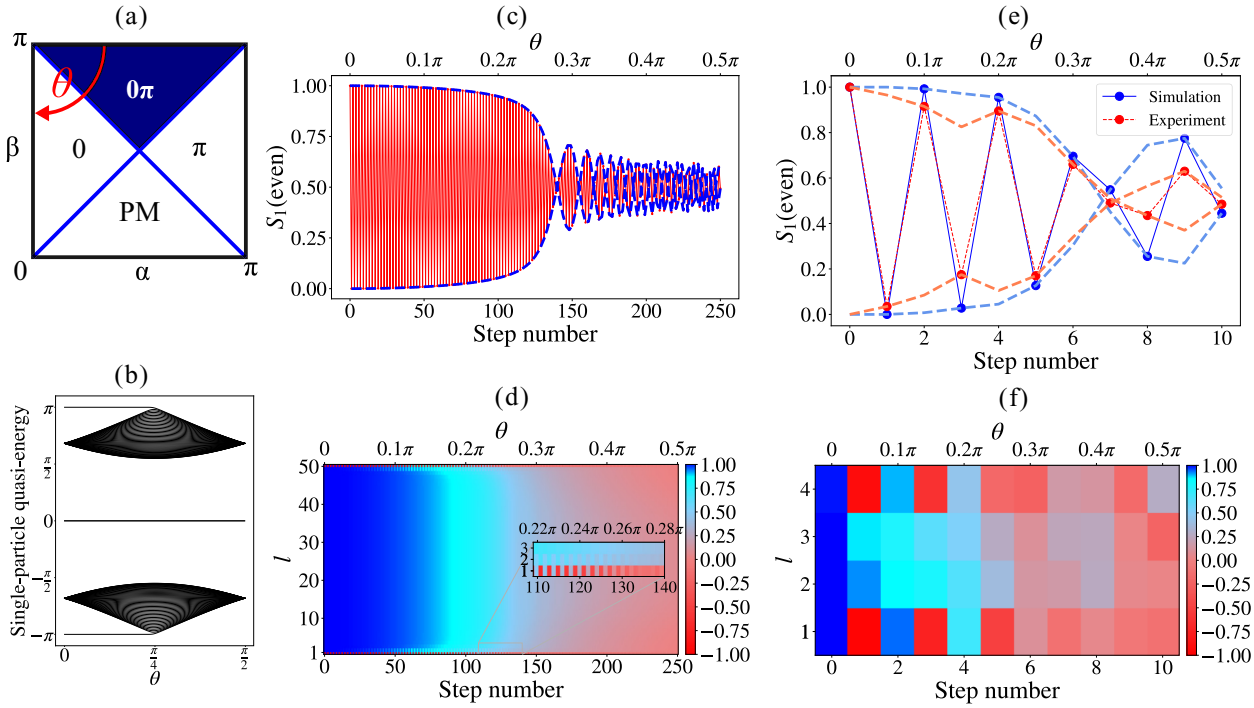

FIG. 2. (a) Phase diagram of the model (7) reproduced from Ref. [40]. The phases PM, 0, π, and 0π are, respectively, the paramagnet, ferromagnet, time crystal, and topological phase. Dark blue represents the topological phase exhibiting SRE switching. The red curve indicates the adiabatic path which we transverse in N_{steps} steps. (b) Single-particle quasienergy spectrum along the path in (a) exhibiting a π mode for $\theta \leqslant \pi/4$. (c), (d) Exact calculation of subsystem parity probability $S_1(\text{even})$ and $\langle X_l \rangle$ for $L = 2L_A = 50$ and $N_{\text{steps}} = 250$. $S_1(\text{even})$ in (c) displays parity switching in the topological (0π) phase up to the phase transition at step $\sim N_{\text{steps}}/2$ followed by a beating structure in the ferromagnetic phase. $\langle X_l \rangle$ in (d) displays edge state parity switching (see inset) in the topological phase. (e), (f) Same quantities as in (c), (d) measured on an ion-based quantum computer on the cloud for $L = 2L_A = 4$ and $N_{\text{steps}} = 10$.

We set $r_0 = 1$ throughout, and initialize the system in the state $|+\rangle = \otimes_l |+\rangle_l$.

The switching of $S_1(\text{even})$ is shown along an adiabatic protocol with $N_{\text{steps}} = 250$ in Fig. 2(c) for a system with $L = 50$ qubits and $L_A = L/2$ [35] (see also Refs. [53–56] therein). Figure 2(d) gives a real-space picture of $\langle X_l \rangle$, showing that for small θ, the edge spins are responsible for the switching. As approaching $\theta = \pi/4$, the extent of the switching zone increases, and eventually the two edges merge at the Floquet topological phase transition.

For $\theta > \pi/4$, $S_1(\text{even})$ gives rise to a beating structure, persisting into the ferromagnetic phase. The frequency of this beating is determined by the difference between two quasienergies of the instantaneous Floquet operator $F(\theta)$. Specifically, our initial state $|+\rangle$ can be combined with the state $Z_1 Z_L |+\rangle$ to form a pair of Floquet eigenstates of $F(\theta = 0)$, denoted by $|1\rangle$ and $|2\rangle$, with quasienergies ω_1 and $\omega_2 = \omega_1 + \pi$. As we vary θ adiabatically, the quasienergies follow their instantaneous values $\omega_{1,2}(\theta)$ [see Fig. 2(b) for the single-particle quasienergies]. In the thermodynamic limit ($L \to \infty$), $\omega_2(\theta) - \omega_1(\theta)$ is pinned to π in the topological phase, giving rise to a periodic switching of $S_1(\text{even})$. For finite systems, there are small deviations, which become significant near the phase transition. Moving into the ferromagnetic phase $\omega_2 - \omega_1$ deviates from π and eventually becomes the energy difference of a domain wall in the ferromagnetic order [35]. This picture allows us to show that the beating amplitude vanishes in the thermodynamic limit as $1/\sqrt{L}$ [35], implying that the parity switching is an FSPT order parameter. The parity switching is observable on a quantum computer as shown in Figs. 2(e) and 2(f) for $L = 4$ and $L_A = L/2$ and $N_{\text{steps}} = 10$ steps (See Ref. [35] for the Amazon Braket quantum algorithm used to generate these plots).

Teleportation through an FSPT phase. The existence of a Floquet operator that switches the symmetry blocks of the reduced density matrix leads to computational power. In the case of SPTs, computation power relies on their entanglement [30,57]. By measuring the state in specific bases, the correlations that compose the entanglement cause the input information to flow. Here, we discuss how FSPT order, with generically unentangled eigenstates, allows teleportation of a quantum state.

We again focus on the simplest case of $G = \mathbb{Z}_2$. Our basic procedure is composed of three steps: (i) Start from a Floquet eigenstate and encode a "qubit" state $|\psi\rangle = \sum_g \alpha_g |g\rangle$ at the left edge in the G-symmetry eigenbasis $|g\rangle = |\pm\rangle$. Encode the identity group element state $|+\rangle$ in the right edge qubit. (ii) Use an ancilla qubit to apply $I + e^{i\chi} F$ with a nonuniversal phase factor $e^{i\chi} = e^{if}$ of the Floquet eigenstate. (iii) Lastly, measure the left edge qubit in the G-symmetry basis. If the FSPT state is nontrivial, then the left edge qubit $|\psi\rangle$ is teleported to the right. This property follows generally for the $\mathbb{Z}_N$ case [35] directly from the algebra in Eqs. (3) and (4) which

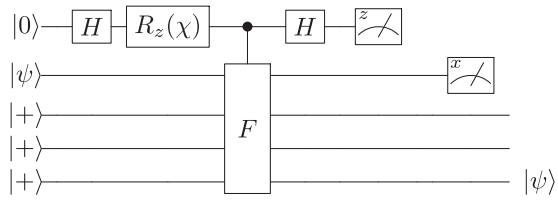

FIG. 3. Teleportation protocol as a probe of FSPT order. A state $|\psi\rangle$ is prepared on the edge. A controlled-F operator followed by a measurement of an ancilla qubit entangles the edge states, allowing for teleportation upon measurement of the first qubit, if and only if F is topological.

defines the action of F and of the symmetry projectors in a given FSPT phase.

This protocol is depicted in Fig. 3 for the point $\theta = 0$ in the topological phase where the edge states are localized on the edge qubits. In this case the initial quantum state is $|\psi\rangle_1 \otimes_{i=2}^{L} |+\rangle_i$, where $|\psi\rangle_1 = \alpha_+|+\rangle_1 + \alpha_-|-\rangle_1$. We have $F = Z_1 Z_L$ (we neglect additional X rotations as those do not change the result) with some additional phase $\chi = \frac{\alpha}{2}(L-2)$. It is easy to see that after applying $I + e^{i\chi} Z_1 Z_L$ and then projecting the left qubit, say to $|+\rangle_1$, the final state is $\otimes_{i=1}^{L-1} |+\rangle_i |\psi\rangle_L$. In Fig. 3 we implement the operator $I + e^{i\chi} F$ using a simple quantum circuit. Adding an ancillary qubit $|0\rangle$ and then acting with Hadamard gate H on it we get the state $\frac{1}{\sqrt{2}}(|0\rangle + |1\rangle)$. Then, we add the phase by rotating around the Z axis with $R_z(\chi) = e^{-i\frac{\chi}{2}Z}$, which takes the ancillary qubit to the state $\frac{1}{\sqrt{2}}(|0\rangle + e^{i\chi}|1\rangle)$. Next, by applying a controlled-F gate, we only apply F on the initial state for the $|1\rangle$ ancilla state, thus, the whole circuit is in the state $\frac{1}{\sqrt{2}}(|0\rangle \otimes |\psi\rangle + |1\rangle \otimes e^{i\chi} F|\psi\rangle)$. Lastly, applying H again on the ancillary qubit, we have $\frac{1}{2}(|0\rangle \otimes [I + e^{i\chi} F]|\psi\rangle + |1\rangle \otimes [I - e^{i\chi} F]|\psi\rangle)$. It is now clear that in the case of measuring the ancilla in the $|0\rangle$ state we implement the operator $I + e^{i\chi} F$ on the initial state. As in MBQC, one can correct for the possible measurement outcomes, and also perform general rotations by measuring in a rotated basis. In order to probe any other point in the FSPT phase, one can apply our adiabatic protocol on the initial state, transforming $\theta = 0 \to \theta_1 < \pi/4$, then apply $I + F(\theta_1) e^{i\chi(\theta_1)}$, and adiabatically evolve back to $\theta = 0$ where the final measurement is done on the first qubit.

Entanglement switching. So far, we considered only unentangled FSPT states with a trivial static cohomology group $\mathcal{H}^2[G, U(1)]$. For nontrivial groups, the Floquet eigenstates contain protected entanglement linked with degeneracies of ρ_A between different symmetry sectors [17]. Consider for example $G = \mathbb{Z}_N \times \mathbb{Z}_N$, where static SPTs are classified by $m \in \mathcal{H}^2[G, U(1)] = \mathbb{Z}_N$ [13] ($m = 0, \ldots, N-1$). In the presence of a Floquet drive classified by an element $c = (c_1, c_2) \in G$ as in Eq. (1), the block $\mathcal{Q}$ turns into $\mathcal{Q} + c$. The degenerate blocks $\mathcal{Q} = (q_1, q_2)$ are grouped into families whose representative is $q' = (q_1', q_2')$, defined mod $\gcd(N, m)$. The entanglement switching of these families is described by $q_i' \to q_i' + c_i \bmod \gcd(N, m)$ ($i = 1, 2$) [35]. We discuss examples of this general formula. If m and N have no common divisors greater than 1, all the symmetry blocks are degenerate and there is no nontrivial switching under the action of F. In contrast, in SPT static phases where $m > 1$ divides N (for example, $m = 2$, $N = 4$) the degeneracy is only partial [17], leading to entanglement, and the degenerate blocks switch from one family to another [35].

Summary. The global topological properties of 1D FSPT phases cannot be revealed by any local measurements in the bulk. Here, we used symmetry resolution measurements to observe the FSPT order, both on a small system realized by a NISQ computer, and analytically on large systems. The latter allowed us to describe a Floquet phase transition into a topologically trivial phase. The topological edge excitations of the Floquet phase adiabatically evolve into domain wall excitations of a ferromagnet. Conversely, this property allows one to prepare adiabatically topological excitations, starting from local excitations. Finally, we demonstrated the ability of FSPT order to teleport a quantum state. All these topological properties, similar to the cohomological classification, hold for periodically driven interacting bosons in general and are not limited to our showcase kicked Ising model which admits a free fermion description.

Acknowledgments. E.S. acknowledges support from ARO (W911NF-20-1-0013), European Research Council (ERC) under the European Unions Horizon 2020 research and innovation programme under Grant Agreement No. 951541, and the U.S.-Israel Binational Science Foundation (Grant No. 2016255). This work was supported by the Israel Science Foundation, Grants No. 151/19 and No. 154/19, and the AWS Cloud Credit for Research Program. We are thankful for discussions with Alon Ron. We acknowledge the use of QUTIP Python library for some of the numerical calculations [58,59].

[1] T. Kitagawa, E. Berg, M. Rudner, and E. Demler, Topological characterization of periodically driven quantum systems, Phys. Rev. B **82**, 235114 (2010).

[2] L. Jiang, T. Kitagawa, J. Alicea, A. R. Akhmerov, D. Pekker, G. Refael, J. I. Cirac, E. Demler, M. D. Lukin, and P. Zoller, Majorana Fermions in Equilibrium and in Driven Cold-Atom Quantum Wires, Phys. Rev. Lett. **106**, 220402 (2011).

[3] M. S. Rudner, N. H. Lindner, E. Berg, and M. Levin, Anomalous Edge States and the Bulk-Edge Correspondence for Periodically Driven Two-Dimensional Systems, Phys. Rev. X **3**, 031005 (2013).

[4] D. V. Else and C. Nayak, Classification of topological phases in periodically driven interacting systems, Phys. Rev. B **93**, 201103(R) (2016).

[5] A. C. Potter, T. Morimoto, and A. Vishwanath, Classification of Interacting Topological Floquet Phases in one Dimension, Phys. Rev. X **6**, 041001 (2016).

[6] C. W. von Keyserlingk and S. L. Sondhi, Phase structure of one-dimensional interacting Floquet systems. I. Abelian symmetry-protected topological phases, Phys. Rev. B **93**, 245145 (2016).

[7] C. W. von Keyserlingk and S. L. Sondhi, Phase structure of one-dimensional interacting floquet systems. II. Symmetry-broken phases, Phys. Rev. B **93**, 245146 (2016).

[8] I.-D. Potirniche, A. C. Potter, M. Schleier-Smith, A. Vishwanath, and N. Y. Yao, Floquet Symmetry-Protected Topological Phases in Cold-Atom Systems, Phys. Rev. Lett. **119**, 123601 (2017).

[9] R. Roy and F. Harper, Abelian Floquet symmetry-protected topological phases in one dimension, Phys. Rev. B **94**, 125105 (2016).

[10] X. Chen, Z.-C. Gu, and X.-G. Wen, Classification of gapped symmetric phases in one-dimensional spin systems, Phys. Rev. B **83**, 035107 (2011).

[11] X. Chen, Z.-C. Gu, and X.-G. Wen, Complete classification of one-dimensional gapped quantum phases in interacting spin systems, Phys. Rev. B **84**, 235128 (2011).

[12] X. Chen, Z.-C. Gu, Z.-X. Liu, and X.-G. Wen, Symmetry-protected topological orders in interacting bosonic systems, Science **338**, 1604 (2012).

[13] X. Chen, Z.-C. Gu, Z.-X. Liu, and X.-G. Wen, Symmetry protected topological orders and the group cohomology of their symmetry group, Phys. Rev. B **87**, 155114 (2013).

[14] F. Pollmann, A. M. Turner, E. Berg, and M. Oshikawa, Entanglement spectrum of a topological phase in one dimension, Phys. Rev. B **81**, 064439 (2010).

[15] E. Cornfeld, L. A. Landau, K. Shtengel, and E. Sela, Entanglement spectroscopy of non-Abelian anyons: Reading off quantum dimensions of individual anyons, Phys. Rev. B **99**, 115429 (2019).

[16] D. Azses, R. Haenel, Y. Naveh, R. Raussendorf, E. Sela, and E. G. Dalla Torre, Identification of Symmetry-Protected Topological States on Noisy Quantum Computers, Phys. Rev. Lett. **125**, 120502 (2020).

[17] D. Azses and E. Sela, Symmetry-resolved entanglement in symmetry-protected topological phases, Phys. Rev. B **102**, 235157 (2020).

[18] C. de Groot, D. T. Stephen, A. Molnar, and N. Schuch, Inaccessible entanglement in symmetry protected topological phases, J. Phys. A: Math. Theor. **53**, 335302 (2020).

[19] M. Goldstein and E. Sela, Symmetry-Resolved Entanglement in Many-Body Systems, Phys. Rev. Lett. **120**, 200602 (2018).

[20] J. C. Xavier, F. C. Alcaraz, and G. Sierra, Equipartition of the entanglement entropy, Phys. Rev. B **98**, 041106(R) (2018).

[21] E. Cornfeld, M. Goldstein, and E. Sela, Imbalance entanglement: Symmetry decomposition of negativity, Phys. Rev. A **98**, 032302 (2018).

[22] R. Bonsignori, P. Ruggiero, and P. Calabrese, Symmetry resolved entanglement in free fermionic systems, J. Phys. A: Math. Theor. **52**, 475302 (2019).

[23] N. Feldman and M. Goldstein, Dynamics of charge-resolved entanglement after a local quench, Phys. Rev. B **100**, 235146 (2019).

[24] D. X. Horváth and P. Calabrese, Symmetry resolved entanglement in integrable field theories via form factor bootstrap, J. High Energy Phys. 11 (2020) 131.

[25] S. Fraenkel and M. Goldstein, Symmetry resolved entanglement: Exact results in 1D and beyond, J. Stat. Mech.: Theory Exp. (2020) 033106.

[26] A. Neven, J. Carrasco, V. Vitale, C. Kokail, A. Elben, M. Dalmonte, P. Calabrese, P. Zoller, B. Vermersch, R. Kueng, and B. Kraus, Symmetry-resolved entanglement detection using partial transpose moments, npj Quantum Inf. **7**, 152 (2021).

[27] S. Fraenkel and M. Goldstein, Entanglement measures in a nonequilibrium steady state: Exact results in one dimension, SciPost Phys. **11**, 085 (2021).

[28] D. V. Else, I. Schwarz, S. D. Bartlett, and A. C. Doherty, Symmetry-Protected Phases for Measurement-Based Quantum Computation, Phys. Rev. Lett. **108**, 240505 (2012).

[29] D. T. Stephen, D.-S. Wang, A. Prakash, T.-C. Wei, and R. Raussendorf, Computational Power of Symmetry-Protected Topological Phases, Phys. Rev. Lett. **119**, 010504 (2017).

[30] R. Raussendorf and H. J. Briegel, A One-Way Quantum Computer, Phys. Rev. Lett. **86**, 5188 (2001).

[31] A. Kumar, P. T. Dumitrescu, and A. C. Potter, String order parameters for one-dimensional Floquet symmetry protected topological phases, Phys. Rev. B **97**, 224302 (2018).

[32] V. Vitale, A. Elben, R. Kueng, A. Neven, J. Carrasco, B. Kraus, P. Zoller, P. Calabrese, B. Vermersch, and M. Dalmonte, Symmetry-resolved dynamical purification in synthetic quantum matter, arXiv:2101.07814.

[33] D. Pérez-García, M. M. Wolf, M. Sanz, F. Verstraete, and J. I. Cirac, String Order and Symmetries in Quantum Spin Lattices, Phys. Rev. Lett. **100**, 167202 (2008).

[34] N. Tantivasadakarn and A. Vishwanath, Symmetric finite-time preparation of cluster states via quantum pumps, arXiv:2107.04019.

[35] See Supplemental Material at http://link.aps.org/supplemental/10.1103/PhysRevB.104.L220301 for proofs of the claims in the Letter, details about the numerical methods, code example for the adiabatic sweeping protocol on a quantum computer on the cloud and additional theoretical explanations based on numerical simulations.

[36] L. Pontrjagin, The theory of topological commutative groups, Ann. Math. **35**, 361 (1934).

[37] E. R. van Kampen, Locally bicompact Abelian groups and their character groups, Ann. Math. **36**, 448 (1935).

[38] Y. G. Berkovich and E. Zhmud, *Characters of Finite Groups. Part 1*, Translations of Mathematical Monographs Vol. 172 (American Mathematical Society, Providence, RI, 1998).

[39] N. Laflorencie and S. Rachel, Spin-resolved entanglement spectroscopy of critical spin chains and Luttinger liquids, J. Stat. Mech.: Theory Exp. (2014) P11013.

[40] V. Khemani, A. Lazarides, R. Moessner, and S. L. Sondhi, Phase Structure of Driven Quantum Systems, Phys. Rev. Lett. **116**, 250401 (2016).

[41] D. A. Abanin, W. De Roeck, and F. Huveneers, Theory of many-body localization in periodically driven systems, Ann. Phys. **372**, 1 (2016).

[42] D. A. Abanin, E. Altman, I. Bloch, and M. Serbyn, Colloquium: Many-body localization, thermalization, and entanglement, Rev. Mod. Phys. **91**, 021001 (2019).

[43] Y. Bahri, R. Vosk, E. Altman, and A. Vishwanath, Localization and topology protected quantum coherence at the edge of hot matter, Nat. Commun. **6**, 7341 (2015).

[44] T.-C. Yen, R. A. Lang, and A. F. Izmaylov, Exact and approximate symmetry projectors for the electronic structure problem on a quantum computer, J. Chem. Phys. **151**, 164111 (2019).

[45] D. V. Else, B. Bauer, and C. Nayak, Floquet Time Crystals, Phys. Rev. Lett. **117**, 090402 (2016).

[46] R. Verresen, R. Moessner, and F. Pollmann, One-dimensional symmetry protected topological phases and their transitions, Phys. Rev. B **96**, 165124 (2017).

[47] B. Friedman, A. Rajak, and E. G. Dalla Torre, Complete characterization of spin chains with two Ising symmetries, Europhys. Lett. **125**, 10008 (2019).

[48] V. Khemani, R. Moessner, and S. L. Sondhi, A brief history of time crystals, arXiv:1910.10745.

[49] J. Zhang, P. Hess, A. Kyprianidis, P. Becker, A. Lee, J. Smith, G. Pagano, I.-D. Potirniche, A. C. Potter, A. Vishwanath *et al.*, Observation of a discrete time crystal, Nature (London) **543**, 217 (2017).

[50] M. Ippoliti, K. Kechedzhi, R. Moessner, S. L. Sondhi, and V. Khemani, Many-Body Physics in the NISQ Era: Quantum Programming a Discrete Time Crystal, PRX Quantum **2**, 030346 (2021).

[51] P. Frey and S. Rachel, Realization of a discrete time crystal on 57 qubits of a quantum computer, arXiv:2105.06632.

[52] X. Mi, M. Ippoliti, C. Quintana, A. Greene, Z. Chen, J. Gross, F. Arute, K. Arya, J. Atalaya, R. Babbush *et al.*, Observation of time-crystalline eigenstate order on a quantum processor, arXiv:2107.13571.

[53] A. Y. Kitaev, Unpaired majorana fermions in quantum wires, Phys. Usp. **44**, 131 (2001).

[54] R. Aguado, Majorana quasiparticles in condensed matter, Riv. Nuovo Cimento **40**, 523 (2017).

[55] B. M. Terhal and D. P. DiVincenzo, Classical simulation of noninteracting-fermion quantum circuits, Phys. Rev. A **65**, 032325 (2002).

[56] M. Wimmer, Algorithm 923: Efficient numerical computation of the Pfaffian for dense and banded skew-symmetric matrices, ACM Trans. Math. Softw. **38**, 1 (2012).

[57] R. Raussendorf, D.-S. Wang, A. Prakash, T.-C. Wei, and D. T. Stephen, Symmetry-protected topological phases with uniform computational power in one dimension, Phys. Rev. A **96**, 012302 (2017).

[58] J. Johansson, P. Nation, and F. Nori, QuTiP: An open-source python framework for the dynamics of open quantum systems, Comput. Phys. Commun. **183**, 1760 (2012).

[59] J. Johansson, P. Nation, and F. Nori, QuTiP 2: A Python framework for the dynamics of open quantum systems, Comput. Phys. Commun. **184**, 1234 (2013).